Pergamon

Int. J. Heat Mass Transfer. Vol. 40, No. 6, pp. 1251–1260, 1997

0017–9310/97 $17.00+0.00

PII: S0017–9310(96)00181–0

Effect of viscous dissipation on a non-Darcy natural convection regime

P. V. S. N. MURTHY and P. SINGH
Department of Mathematics, Indian Institute of Technology, Kanpur 208016, India

(*Received for publication* 18 *June* 1996)

Abstract—The effect of viscous dissipation on non-Darcy natural convection flow along an isothermal vertical wall embedded in a saturated porous medium is initiated. The flow field is divided into non-Darcy $G = 0$, intermediate $G = 0(1)$, and limit Darcy regimes $G \to \infty$ using the inertia–buoyancy scales. Thermal dispersion effects are also taken into consideration. It is observed that the viscous dissipation effect reduces the heat transfer rate by about 10% in all three flow regimes. It is also found that the effect of viscous dissipation is greater as the value of the parameter G increases. The effect of viscous dissipation in all three flow regimes increases with the dispersion parameter. Copyright © 1996 Elsevier Science Ltd.

1. INTRODUCTION

Natural convection flow and heat transfer in a saturated porous media has gained much attention during the past two decades because of its wide range of applications in packed bed reactors, porous insulation, beds of fossil fuels, nuclear waste disposal, usage of porous conical bearings in lubrication technology, geophysics and energy related engineering problems. A good review of buoyancy driven boundary-layer flows in a Darcian fluid is given in Nield and Bejan [1]. When the pore Reynolds number is high enough for the Darcy flow model to breakdown, Plumb and Huenefeld [2] studied the fundamental problem of non-Darcy natural convection from heated vertical walls in a saturated porous medium. Later Bejan and Poulikakos [3] and Bejan [4], by dividing the flow regime into non-Darcy and intermediate regimes, studied the same problem using fluid inertia–buoyancy scaling and defined large Reynolds-number-limit Rayleigh number Ra_∞. The new dimensionless group G defined in their analysis has been understood to be the number which describes the "extent to which the flow departs from Darcy law" by their successor, Fand *et al.* [5]. The non-similar boundary-layer equations resulting from the Forchheimer natural convection with power law wall variation were solved by Chen and Ho [6].

In the case when inertia effects are prevalent, the transverse thermal dispersion effects will become important, and the analysis is dealt with at length in works by Plumb [7], Cheng [8], Hong and Tien [9], Hong *et al.* [10], Cheng and Vortmeyer [11], Amiri and Vafai [12] etc. All these works confirm the importance of the thermal dispersion effect. Except for Cheng and Vortmeyer [11], all other works use the linear dependence of dispersion diffusivity on streamwise velocity. In order to correlate the available experimental data concerning the packed beds, Cheng and Vortmayer [11] introduced a wall function term into the term of dispersion diffusivity.

The effect of viscous dissipation on natural convection in fluids has been studied by Gebhart [13] for power law vertical wall variation. He obtained a perturbation solution in terms of a parameter which could not be expressed in terms of either the Rayleigh number or the Prandtl number, and observed its increasing effect as the Prandtl number increases. Later Gebhart and Mollendorf [14] obtained the similarity solution for the same problem when exponential wall temperature variation is used and a similar trend was observed. A comment was made by Fand and Brucker [15] that the effect of viscous dissipation might be significant in the case of natural convection in porous medium in connection with their experimental correlation for heat transfer in external flows. The validity of the comment was tested for the Darcy model by Fand *et al.* [5], both experimentally and analytically while estimating the heat transfer coefficient from a horizontal cylinder embedded in a saturated porous medium. Their mathematical analysis is confined to studying the dissipation effect using a steady, 1-D energy equation, the basis of the equation is from the analogy given by Bejan [16] for the inclusion of viscous dissipation effects. The influence of viscous dissipation can be seen from the analogy given by Tucker and Dessenberger [17] to model the heat transfer and fluid flow through porous media in order to study the resin transfer molding (R.T.M.) for producing fiber reinforced polymeric parts in final shape. Recently, Nakayama and Pop [18] studied the effect of viscous dissipation on the Darcian free convection over a non-isothermal body of arbitrary shape embedded in a saturated porous medium using the integral method. Their results indicated that viscous dissipation lowers the rate of heat transfer.

NOMENCLATURE

b	empirical constant of the porous medium
c_p	specific heat at constant pressure
d	pore or particle diameter
Ds	dispersion parameter $\gamma Ra_d^{1/2}$
f	dimensionless stream function
f_m	stream function components
$\mathbf{g}$	gravitational vector
g	gravitational constant
G	non-dimensional group $\nu/\mathrm{K}\{bg\beta\theta_w\}^{-1/2}$
Ge_x	Gebhart number $g\beta x/c_p$
K	permeability
k_e	effective thermal conductivity
Nu	Nusselt number
p	pressure
q	local speed of the fluid
Ra_x	local Rayleigh number $g\beta\theta_w x^2/b\alpha^2$
Ra_d	Rayleigh number based on particle diameter $g\beta\theta_w d^2/b\alpha^2$
T	temperature
t_m	temperature components
$\mathbf{V}$	velocity vector
u	velocity component in streamwise direction
v	velocity component in cross-stream direction
x	streamwise coordinate
y	cross-stream coordinate.

Greek symbols

α_e	effective thermal diffusivity
α	fluid molecular diffusivity
α_d	dispersion diffusivity
β	thermal expansion coefficient
γ	mechanical dispersion coefficient
η	similarity variable
θ	dimensionless temperature
ψ	streamfunction
ε	perturbation parameter Ge_x
μ	viscosity of the fluid
ν	fluid kinematic viscosity
ρ	fluid density.

Subscripts

w	evaluated at wall condition
∞	evaluated at infinity.

In the present paper, we initiated the study of the effect of viscous dissipation on non-Darcy natural convection in a porous medium. We considered the steady 2-D Forchheimer natural convection flow and heat transfer along an isothermal vertical wall with thermal dispersion and viscous dissipation effects. The scaling proposed by Bejan and Poulikakos [3] is adopted and the effect of viscous dissipation in non-Darcy, intermediate and limit Darcy regimes is studied with and without thermal dispersion effects. The results show a significant decrease in the heat transfer rate with the inclusion of the viscous dissipation effect. It is seen that as the value of the dispersion parameter increases, the effect of viscous dissipation increases in all three regimes and the percentage decrease in the value of $Nu/Ra_x^{1/4}$ increases with the value of G.

2. GOVERNING EQUATIONS

Consider the problem of natural convection from an isothermal vertical wall embedded in a saturated porous medium, in which the pore Reynolds number is high enough for the departure of the flow from Darcy's law. At higher velocities, inertial effects become appreciable, causing an increase in the form drag, in addition to the bulk damping resistance due to the porous structure. Viscous resistance due to the solid boundary is neglected because the present study is assumed to be valid for low permeability and porosity. So the pressure drop is proportional to the linear combination of flow velocity and the square of the velocity. Both the thermal dispersion and viscous dissipation terms are retained in the energy equation. So, the governing equations for the flow and heat transfer are

$$\nabla\cdot\mathbf{V}=0 \tag{1}$$

$$B(q)\mathbf{V}=\frac{K}{\mu}(-\nabla p+\rho\mathbf{g}) \tag{2}$$

$$(\mathbf{V}\cdot\nabla T)=\nabla\cdot(\alpha_e\nabla T)+\frac{1}{\rho c_p}\mathbf{V}(-\nabla p+\rho\mathbf{g}) \tag{3}$$

$$\rho=\rho_\infty[1-\beta(T-T_\infty)] \tag{4}$$

where

$$B(q)=\left(1+\frac{bK\rho}{\mu}q\right).$$

Making use of the momentum equation in the energy equation, the viscous dissipation term can be modified as

$$(\mathbf{V}\cdot\nabla T)=\nabla\cdot(\alpha_e\nabla T)+\frac{\nu}{Kc_p}B(q)(\mathbf{V})^2. \tag{5}$$

The boundary conditions are

$$\left.\begin{aligned} y=0 \quad & v=0 \quad \text{and} \quad T=T_w \\ y\to\infty \quad & u=0 \quad \text{and} \quad T\to T_\infty \end{aligned}\right\}. \tag{6}$$

In the above equations, $\mathbf{V}$ is the velocity vector, q is the local speed, K is the permeability, μ is the viscosity,

p is the pressure, ρ is density, $\mathbf{g}$ is the gravity vector, T is the temperature, α_e is the effective thermal diffusivity, c_p is the specific heat at constant pressure, β is the coefficient of thermal expansion and b is the empirical constant of the porous medium. Eliminating pressure and making use of the boundary-layer and Boussenesq approximations, in equations (1), (2) and (5), we get

$$\frac{\partial u}{\partial x}+\frac{\partial v}{\partial y}=0 \tag{7}$$

$$\frac{\partial u}{\partial y}+\frac{bK\rho}{\mu}\frac{\partial u^2}{\partial y}=\frac{Kg\beta\rho}{\mu}\frac{\partial T}{\partial y} \tag{8}$$

$$u\frac{\partial T}{\partial x}+v\frac{\partial T}{\partial y}=\frac{\partial}{\partial y}\left[(\alpha+\gamma\,\mathrm{d}u)\frac{\partial T}{\partial y}\right]+\frac{v}{Kc_p}u\left(u+\frac{bK\rho}{\mu}u^2\right). \tag{9}$$

In arriving at the above equations, we made use of the simplifications via:

- $uq = u(u^2+v^2)^{1/2} = u^2(1+v^2/u^2)^{1/2} \approx u^2$ under the boundary-layer approximations;
- $\partial p/\partial y = 0$ inside the boundary layer, so the term $v/Kc_p\, v\,(-\partial p/\partial y)$ vanishes in the energy equation;
- $\alpha_e = \alpha+\alpha_d$, α is the stagnant diffusivity, and the dispersion diffusivity α_d is assumed to vary linearly with the streamwise velocity component, $\alpha_d = \gamma\,\mathrm{d}u$.

The resulting boundary layer equations (7)–(9), along with the boundary conditions are solved using the perturbation technique. We made use of the scales proposed in Bejan and Poulikakos [3] for the flow field and boundary layer thickness. Then the transformations for converting the partial differential equations into non-similar ordinary differential equations are given as:

$$\eta=\frac{y}{x}Ra_x^{1/4} \tag{10}$$

$$\psi=\alpha Ra_x^{1/4}f(x,\eta) \tag{11}$$

$$T-T_\infty=(T_w-T_\infty)\theta(x,\eta). \tag{12}$$

Here $Ra_x=g\beta\theta_w x^2/b\alpha^2$ and $\theta_w=T_w-T_\infty$. ψ is the stream function defined so that $u=\mathrm{d}\psi/\mathrm{d}y$, $v=-\mathrm{d}\psi/\mathrm{d}x$ and the equation of continuity is satisfied automatically. This transformation reduces equations (7)–(9) into

$$Gf''+2f'f''=\theta' \tag{13}$$

$$\theta''+\frac{1}{2}f\theta'+\gamma Ra_d^{1/2}(f''\theta'+f'\theta'')+Ge_x f'(Gf'+f'^2)=x\left(f'\frac{\partial\theta}{\partial x}-\theta'\frac{\partial f}{\partial x}\right) \tag{14}$$

where $G=\nu/K(bg\beta\theta_w)^{-1/2}$, $Ra_d=g\beta\theta_w d^2/b\alpha^2$ and $Ge_x=g\beta x/c_p=\varepsilon$ the dissipation parameter (we chose it for the sake of perturbation) and $\gamma Ra_d^{1/2}=Ds$ is the dispersion parameter. Using the integrated form of equation (13), the energy equation becomes

$$\theta''+\tfrac{1}{2}f\theta'+Ds(f''\theta'+f'\theta'')+\varepsilon f'\theta=\varepsilon(f'\theta_\varepsilon-\theta' f_\varepsilon). \tag{15}$$

In all the equations the superscript $'$ represents the differentiation with respect to η and subscript ε represents the differentiation with respect to ε. The boundary conditions become

$$\left.\begin{array}{ll}\eta=0 & f(\varepsilon,0)=0 \quad\text{and}\quad \theta(\varepsilon,0)=1\\ \eta\to\infty & f'(\varepsilon,\infty)=0 \quad\text{and}\quad \theta(\varepsilon,\infty)=0\end{array}\right\}. \tag{16}$$

Now writing the non-dimensional streamfunction and temperature function in terms of perturbation functions f_m and t_m as

$$\left.\begin{aligned}f(\varepsilon,\eta)&=\sum_{m=0}^{\infty}(-1)^m\varepsilon^m f_m(\eta)\\ \theta(\varepsilon,\eta)&=\sum_{m=0}^{\infty}(-1)^m\varepsilon^m t_m(\eta)\end{aligned}\right\}. \tag{17}$$

Substituting equations (17) into equations (13) and (15) and equating the various coefficients of powers of ε to zero (here we collected terms up to the second power of ε), we are left with the following sets of ordinary differential equations:

ε^0

$$\left.\begin{aligned}Gf_0''+2f_0'f_0''-t_0'&=0\\ t_0''+\tfrac{1}{2}f_0t_0'+Ds(f_0''t_0'+f_0't_0'')&=0\end{aligned}\right\} \tag{18}$$

with the corresponding boundary conditions

$$f_0(0)=f_0'(\infty)=t_0(0)-1=t_0(\infty)=0$$

ε^1

$$\left.\begin{aligned}Gf_1''+2f_0'f_1''+2f_0''f_1'-t_1'&=0\\ t_1''+\tfrac{1}{2}(f_0t_1'+t_0'f_1)+Ds(f_0''t_1'+f_1''t_0'+f_0't_1''&\\ +f_1't_0'')+f_0't_0-(f_0't_1-f_1't_0')&=0\end{aligned}\right\} \tag{19}$$

with the corresponding boundary conditions

$$f_1(0)=f_1'(\infty)=t_1(0)=t_1(\infty)=0$$

ε^2

$$\left.\begin{aligned}&Gf_2''+2(f_0'f_2''+f_1'f_1''+f_2'f_0'')-t_2'=0\\ &t_2''+\tfrac{1}{2}(f_0t_2'+f_1t_1'+f_2t_0')+Ds(f_0''t_2'\\ &+f_1''t_1'+f_2''t_0'+f_0't_2''+f_1't_1''+f_2't_0'')\\ &-(f_0't_1+f_1't_0)+(f_1t_1'+2f_2t_0'-2f_0't_2-f_1't_1)=0\end{aligned}\right\} \tag{20}$$

with the corresponding boundary conditions

$$f_2(0)=f_2'(\infty)=t_2(0)=t_2(\infty)=0$$

etc.

Table 1. Decrease in Nusselt number with ε when $Ds = 0$; $\infty = 100$ (here)

G	$f'(0)$	t'_0	t'_1	t'_2	$Nu/Ra_x^{1/4} = -\theta'(0)$ $\varepsilon = 0$	$\varepsilon = 0.01$	$\varepsilon = 0.1$
0	1.0	−0.4941	−0.5161	0.0904	0.4941	0.4889	0.4416
0.1	0.9512	−0.4778	−0.5013	0.0881	0.4778	0.4728	0.4268
1.0	0.6180	−0.3658	−0.3904	0.0695	0.3658	0.3619	0.3261
10	0.0990	−0.1402	−0.1506	0.0272	0.1402	0.1387	0.1249
∞	0.0100	−0.0460	−0.0468	0.0082	0.0460	0.0455	0.0412

3. RESULTS AND DISCUSSION

The first set of ordinary differential equations (equation (18)) i.e. the zero dissipation problem with $Ds = 0$, is the problem considered in Bejan and Poulikakos [3]. The present analysis covers two cases:

- the effect of thermal dispersion in the non-Darcy regime ($G = 0$) and in the limit Darcy regime ($G \to \infty$);
- The effect of viscous dissipation in the non-Darcy regime and in the limit Darcy regimes with and without thermal dispersion effects.

The sets of differential equations (18)–(20) are solved successively, by giving appropriate initial guess values for $f'_i(0)$, $t'_i(0)$, $i = 0, 1, 2$ to match the values with the corresponding boundary conditions at $f'_i(\infty)$, $t_i(\infty)$, $i = 0, 1, 2$. NAG software is used for integrating the corresponding first order system of equations (18)–(20) and shooting and matching the initial and boundary conditions and the results are observed up to an accuracy of 5.0×10^{-6}. The results which cover the above two cases are presented in Tables 1 and 2.

Table 1 gives the influence of viscous dissipation on non-Darcy, intermediate and limit Darcy regimes when the effect of thermal dispersion is neglected. Table 2 gives the influence of viscous dissipation in the three regimes as the value of Ds increases. The percentage decrease in the Nusselt number results for two values of the viscous dissipation parameter from zero dissipation values is also shown in the Table 3.

From the results obtained, it is observed that the values of $f'_i(0) = 0, i = 1, 2$ and $f'_i(\infty) = 0, i = 0, 1, 2$. So there is no change in the value of $f'(0)$ which is equal to $f'_1(0)$ for all values of the parameter G and from Fig. 1, it can be observed that the effective vertical velocity

$$f'(\eta) = f'_0(\eta) - \varepsilon\, f'_1(\eta) + \varepsilon^2 f'_2(\eta)$$

(at $\varepsilon = 0.1$, shown as dashed curves) thickens a little from its zero dissipation component, i.e. $f'(\eta) = f'_0(\eta)$ and this deviation increases with an increase in the value of the dissipation parameter, when $G = 0.1$, $G = 10$ are plotted. In Figs. 2 and 3 the vertical velocity components $f'_i(\eta)$, $i = 0, 1, 2$ are plotted for

Table 2. Decrease in Nusselt number with ε and Ds; $\infty = 100$ (here)

G	Ds	$-t'_0$	$-t'_1$	t'_2	$-\theta'(0)$ $\varepsilon = 0$	$\varepsilon = 0.01$	$\varepsilon = 0.1$	$Nu/Ra_x^{1/4}$ $\varepsilon = 0$	$\varepsilon = 0.01$	$\varepsilon = 0.1$
0	0.2	0.444	0.4656	0.0819	0.444	0.4393	0.3966	0.5328	0.5272	0.4759
	2.0	0.2666	0.2837	0.0510	0.2666	0.2637	0.2377	0.7998	0.7913	0.7132
	5.0	0.1863	0.1968	0.0351	0.1863	0.1843	0.1663	1.1178	1.1059	0.9976
0.1	0.2	0.4311	0.4541	0.0802	0.4311	0.4265	0.3849	0.5131	0.5077	0.4581
	2.0	0.2617	0.2798	0.0502	0.2617	0.2590	0.2332	0.7596	0.7514	0.6769
	5.0	0.1821	0.1959	0.0353	0.1821	0.1802	0.1622	1.0482	1.0369	0.9334
	10.0	0.1335	0.144	0.026	0.1335	0.1321	0.1188	1.4034	1.3882	1.2393
1.0	0.2	0.3406	0.3645	0.0652	0.3406	0.3369	0.3035	0.3827	0.3786	0.3410
	2.0	0.2280	0.2474	0.0449	0.2280	0.2255	0.2028	0.5098	0.5043	0.4535
	5.0	0.1637	0.1791	0.0327	0.1637	0.1619	0.1455	0.6695	0.6621	0.5949
	10.0	0.1216	0.1336	0.0245	0.1216	0.1203	0.1080	0.8731	0.8635	0.7754
10.0	0.2	0.1384	0.1488	0.0269	0.1384	0.1369	0.1233	0.1411	0.1396	0.1257
	2.0	0.1251	0.1351	0.0245	0.1251	0.1238	0.1114	0.1499	0.1483	0.1334
	5.0	0.1093	0.1186	0.0217	0.1093	0.1081	0.0972	0.1634	0.1616	0.1454
	10.0	0.0923	0.1008	0.0185	0.0923	0.0913	0.0820	0.1837	0.1817	0.1632
∞	0.2	0.0459	0.0467	0.0082	0.0459	0.0454	0.0411	0.0460	0.0455	0.0412
	2.0	0.0454	0.0462	0.0081	0.0454	0.0450	0.0407	0.0463	0.0458	0.0415
	5.0	0.0446	0.0454	0.0080	0.0446	0.0441	0.0399	0.0468	0.0463	0.0420
	10.0	0.0433	0.0441	0.0078	0.0433	0.0429	0.0388	0.0476	0.0471	0.0427

Table 3. Percentage decrease in Nusselt number with ε and Ds

G	Ds	Percentage decrease when $\varepsilon = 0.01$	Percentage decrease when $\varepsilon = 0.1$
0	0	1.04635	10.62821
	0.2	1.05106	10.67098
	2.0	1.06276	10.83270
0.1	0	1.05065	10.67601
	0.2	1.05243	10.71721
	2.0	1.07009	10.88392
	5.0	1.0809	10.95401
1.0	0	1.06615	10.86248
	0.2	1.07133	10.89626
	2.0	1.08079	11.04920
	5.0	1.09186	11.13517
	10.0	1.0984	11.18900
10.0	0	1.07704	10.93438
	0.2	1.09112	10.94657
	2.0	1.08093	10.99619
	5.0	1.08323	11.04651
	10.0	1.09436	11.11776

$Ds = 0$ and $Ds = 10$. From Fig. 2, the curve representing f'_1 is seen to be more effective for the value of $G = 0.1$ and it becomes thin as we move into the intermediate regime. The slope of the curve f'_1 for $G = 0.1$ is maximum at $\eta = 1.07$ (approximately) and this value of η increases to 3.8 for the same curve when the dispersion parameter is increased to $Ds = 10$ (Fig. 3) i.e. the effect of dissipation is more widely spread as the value of Ds increases.

The evolution of the vertical component of velocity plotted in Figs. 1–3 with G is understood in the following way: the parameter G is only equal to $Gr^{-1/2}$ where $Gr = K^2 b g \beta \theta_w / \nu^2$ is the modified Groshaff number which gives the relative importance of the inertial effects and when the Ergun model is used in evaluating the constants in the Forchheimer flow model, $Gr = Gr'$ becomes $K' K g \beta \theta_w / \nu^2$ which was the controlling parameter in the study of Plumb and Huenefeld [2]. Replacing G by $Gr^{-1/2}$ in equation (13), we get $f' + Gr^{1/2} f'^2 = Gr^{1/2}\theta$. When Gr is large (i.e. inertial effects are more) the first term in the above equation can be comfortably dropped and a close look at the boundary condition $\theta(0) = 1$ gives $f'(0) = 1$. So the evolution of vertical velocity starts from $f'(0) = 1$ at $G = 0$ and as we move into the intermediate regime $G = 0(1)$ specifically at $G = 1.0$, the term f' cannot be neglected in the above equation and for $f'(0) = 0.618$ and $\theta'(0) = -0.3658$ the same values were observed in the analysis of Plumb and Huenefeld [2] for $Gr' = 1$, (see Table 4) when $Ds = 0$, and $\varepsilon = 0$. Similarly the non-dimensional temperature distribution for $t_i(0)$, $i = 0, 1, 2$ is plotted in Figs. 4 and 5 for $Ds = 0$ and $Ds = 10$, respectively. From Fig. 6, it can be observed that the effect of viscous dissipation increases as the

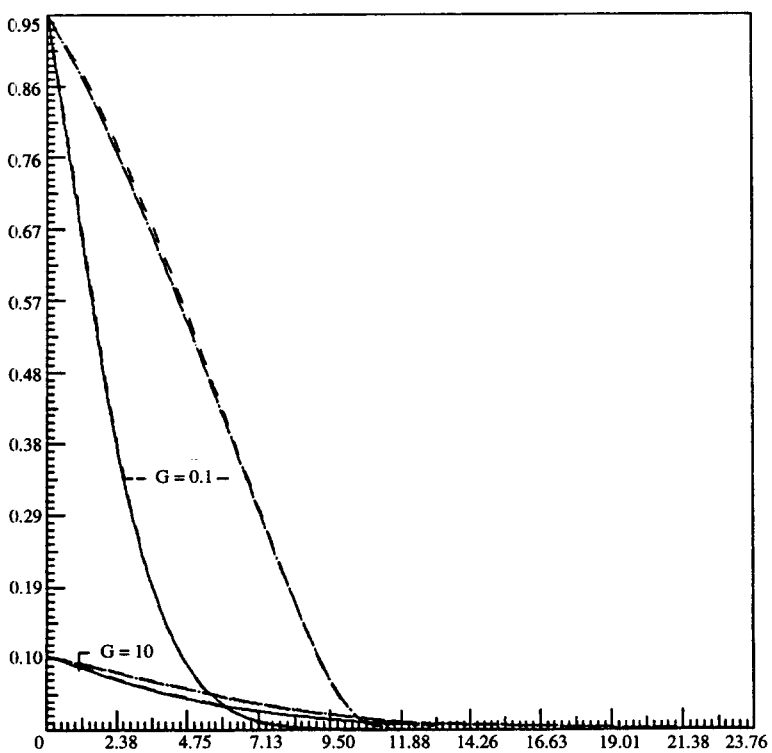

Fig. 1. Deviation of vertical velocity profiles f' vs η (dashed curves) from its zero dissipation profiles $f'_0(\eta)$ vs η for $G = 0.1$, 10, when $Ds = 0$ (solid curves) and $Ds = 10$ (dash-dot curves) (when $\varepsilon = 0.1$).

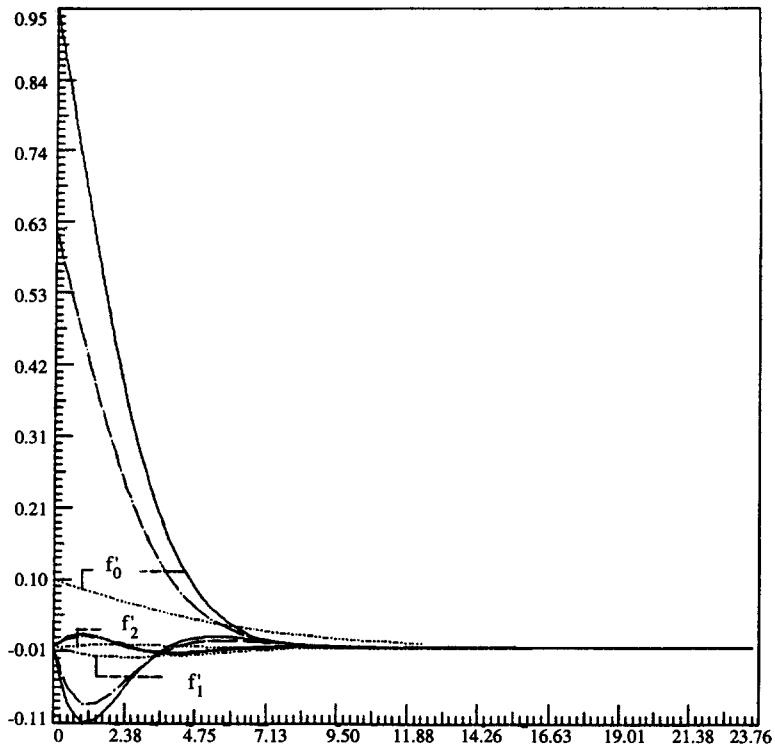

Fig. 2. Vertical velocity components $f_i'(\eta)$ vs η, $i = 0, 1, 2$ for $G = 0.1$ (solid curves), $G = 1.0$ (dash-dot curves), and $G = 10.0$ (dotted curves) when $Ds = 0$.

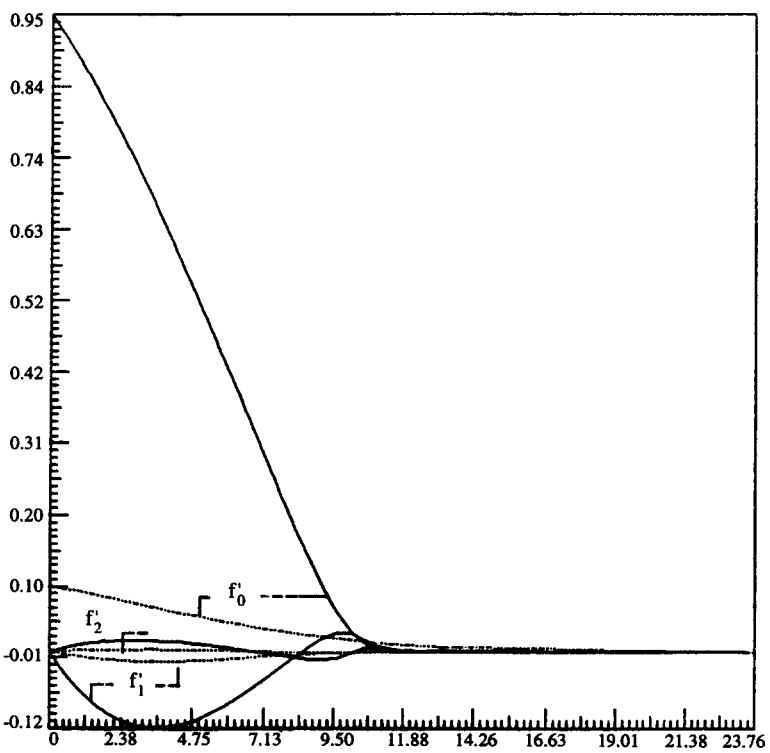

Fig. 3. Vertical velocity components $f_i'(\eta)$ vs η, $i = 0, 1, 2$ for $G = 0.1$ (solid curves), and $G = 10.0$ (dotted curves) when $Ds = 10$.

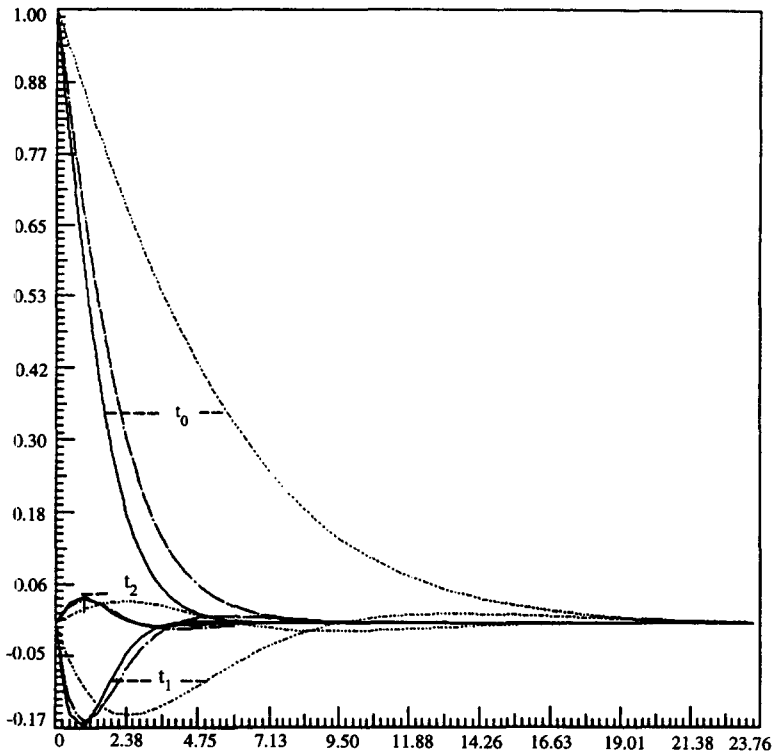

Fig. 4. Temperature components $t_i(\eta)$ vs η, $i = 0, 1, 2$ for $G = 0.1$ (solid curves), $G = 1.0$ (dash-dot curves) and $G = 10.0$ (dotted curves) when $Ds = 0$.

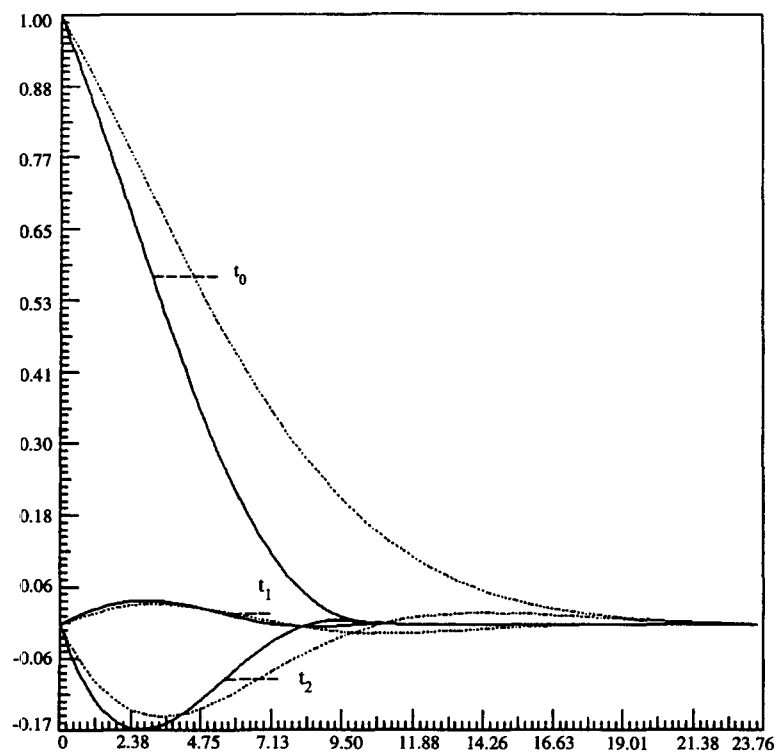

Fig. 5. Temperature components $t_i(\eta)$ vs η, $i = 0, 1, 2$ for $G = 0.1$ (solid curves), $G = 10.0$ (dotted curves) when $Ds = 10.0$.

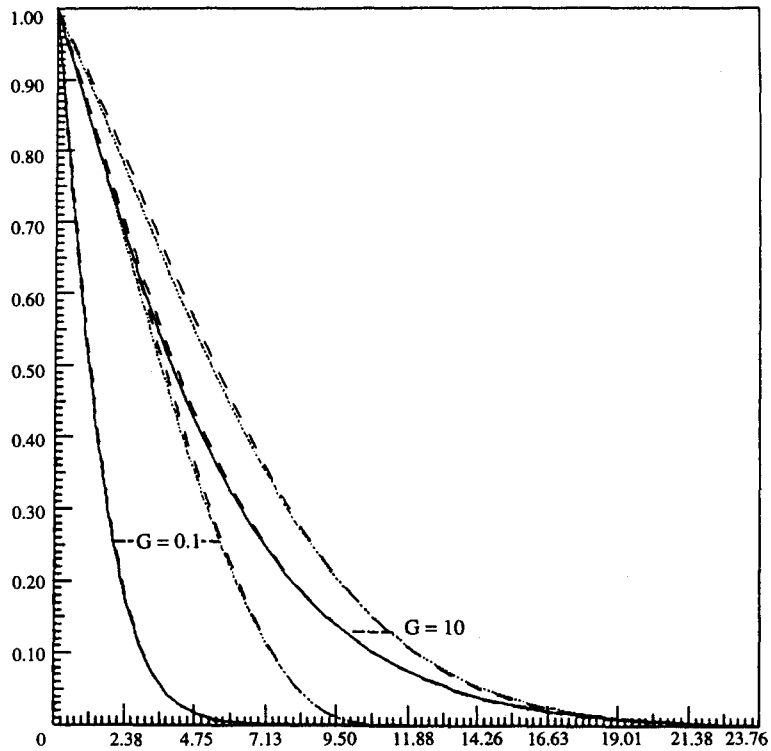

Fig. 6. Deviation of temperature profiles $\theta(\eta)$ vs η (dashed curves) from its zero dissipation profiles $t_0(\eta)$ vs η when $Ds = 0$ (solid curves) and $Ds = 10$ (dotted curves) (when $\varepsilon = 0.1$).

value of G increases, and it has a pronounced effect as the value of the thermal dispersion parameter increases. The dashed curves correspond to the effective temperature distribution obtained from equation (17) at $\varepsilon = 0.1$.

Since we have used a series solution for solving the problem and so the streamwise derivatives of the dependent variables are not neglected in the governing equations the results obtained here must be very appropriate. The values for $t_1'(0)$ and $t_2'(0)$ are significant, and the trend shows that even if we consider more terms in the series expansion for f and θ (i.e. after the second level of perturbation), the resulting values for $t_3'(\eta)$ etc. and their contribution (i.e. $-\varepsilon^3 t_3'(\eta)+\varepsilon^4 t_4'(\eta)-\ldots$) will be very small in the range of the values of ε for which the series solution is valid. The values of $-\theta'(\eta)$ (dotted curves) are plotted for $G = 0.1$ and $G = 10$ with an increase in the dispersion parameter in Fig. 7. The solid curves correspond to the zero dissipation curves of $-\theta'$ i.e. $-t_0'(0)$ and the dotted curves correspond to effective temperature gradients (negative) when $\varepsilon = 0.1$ i.e.

$$\theta'(\eta) = t_0'(\eta) - \varepsilon t_1'(\eta) + \varepsilon^2 t_2'(\eta).$$

When $Ds = 0$, the values of $-t_0'(\eta)$ decreases with η steadily, whereas the value of the dispersion parameter increases, $-t_0'(\eta)$ increases up to a certain value of η and then returns to zero; the reasons for this are well explained in Hong and Tien [9]. Consideration of viscous dissipation reveals that the increase in temperature gradient $-\theta'$ is greater near the wall region in the non-Darcy regime when $Ds = 0$, and this peak is smoothed as we go into the inter-

Table 4. Nusselt number correlation using equation (21)

$Gr' = G^{-2}$ / Gr'	$-\theta'(0)$ ref. [1]	$-\theta'(0)$ equation (21)	$-\theta'(0)$ present analysis	$-\theta'(0)$ ref. [2]
0.01	0.44232	0.13987	0.1402	—
0.04	0.4376	0.1957	—	0.1980
0.1	0.42969	0.24163	0.2421	—
1.0	0.36617	0.36617	0.3658	0.3700
10.0	0.25126	0.44681	0.4457	—
25.0	0.2076	0.46421	0.4625	0.4630
100.0	0.15186	0.4802	0.4778	—

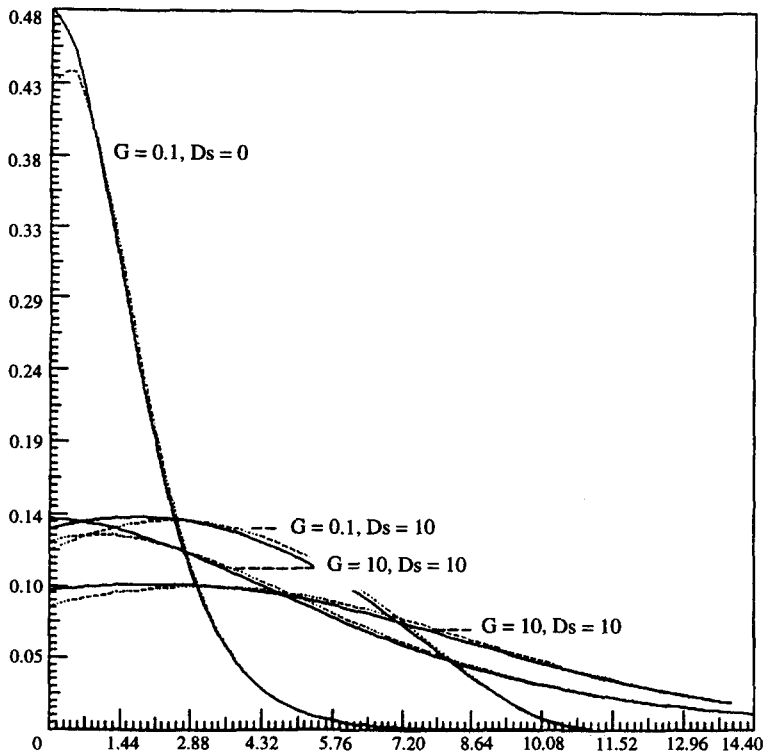

Fig. 7. $-t_0'(\eta)$ vs η (solid curves) $-\theta'(\eta)$ vs η (dotted curves).

mediate regime and with the increasing values of G and Ds. Now the local heat transfer rate from the surface of the plate to the medium is given by

$$q = -k_e \frac{dT}{dy}_{y=0}$$

where k_e is the effective thermal conductivity which is the sum of the stagnant conductivity and the dispersion conductivity (due to mechanical dispersion). The local Nusselt number Nu_x is given by

$$\frac{Nu}{Ra_x^{1/4}} = [1 + Dsf''(0)]\{-t_0'(\eta) + \varepsilon t_1'(\eta) - \varepsilon^2 t_2'(\eta)\}.$$

The first column under the Nusselt number expression in Table 1 is the solution obtained in Bejan and Poulikakos [3] and the second and third columns correspond to the Nusselt number values when the viscous dissipation parameter ε takes values 0.01 and 0.1. Table 2 gives the combined effect of thermal dispersion and viscous dissipation in all three regimes under consideration. The Nusselt number results for the problem under consideration using the Darcy–buoyancy comparison can be obtained from the correlation equation

$$\frac{Nu}{Ra_x^{1/4}} = \frac{Nu}{Ra^{1/2}}\{Gr'\}^{1/4} \tag{21}$$

where $Ra = Kg\beta\theta_w x/\alpha\nu$, [2]. This equation behaves as a bridge for the Nusselt number which result using the inertia–buoyancy comparison and the Darcy–buoyancy comparison. In Table 4 we compare the values of Nusselt number results obtained using the correlation equation (21) (by making use of ref. [2]) and those obtained by solving directly equation (18) with $Ds = 0$. The thermal dispersion enhances the heat transfer rate, while the viscous dissipation tends to lower it and the values of the percentage decrease in the Nusselt number results given in Table 3 reveal that:

- the effect of viscous dissipation increases as we move from a non-Darcy to a limit Darcy regime;
- the effect of viscous dissipation increases as the value of Ds increases in (a) a non-Darcy regime, (b) an intermediate regime and (c) a limit Darcy regime. Figure 8 gives a clear picture of the influence of viscous dissipation on the Nusselt number. It is seen from Fig. 8 that the effect of dissipation increases with thermal dispersion.

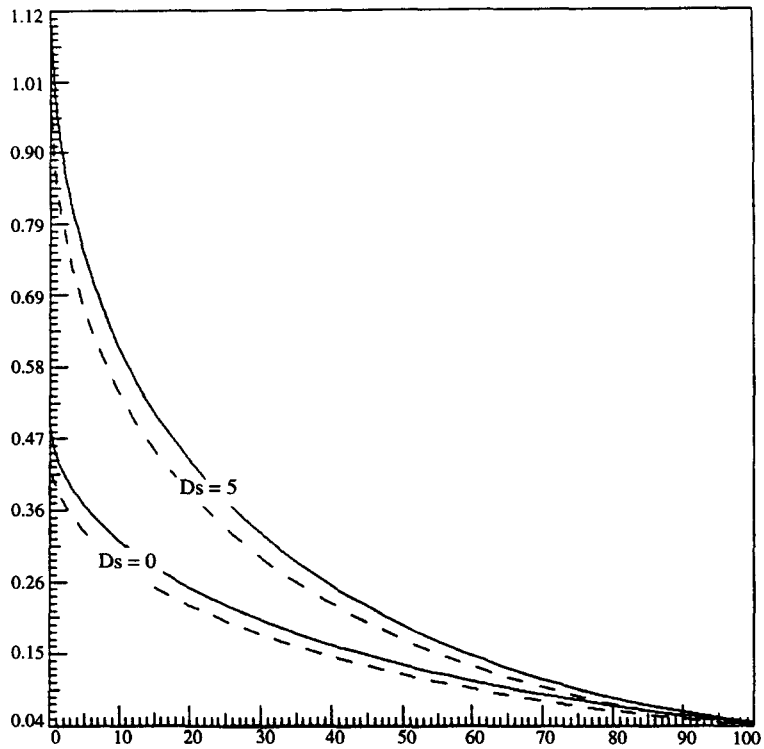

Fig. 8. $Nu/Ra_x^{1/4}$ vs G when $\varepsilon = 0$ (solid curves) and $\varepsilon = 0.1$ (dashed curves).

Acknowledgement—The authors are very grateful to Prof. A. Bejan for his comments and valuable suggestions on this manuscript.

REFERENCES

1. Nield, D. A. and Bejan, A., *Convection in Porous Media*. Springer Verlag, New York, 1992.
2. Plumb, O. and Huenefeld, J. C., Non-Darcy natural convection from heated surfaces in saturated porous medium. *International Journal of Heat and Mass Transfer*, 1981, **24,** 765–768.
3. Bejan, A. and Poulikakos, D., The non-Darcy regime for vertical boundary layer natural convection in a porous medium. *International Journal of Heat and Mass Transfer*, 1984, **27,** 717–722.
4. Bejan, A., The basic scales of natural convection heat and mass transfer in fluids and fluid saturated porous media. *International Communications in Heat and Mass Transfer*, 1987, **14,** 107–123.
5. Fand, R. M., Steinberger, T. E. and Cheng, P., Natural convection heat transfer from a horizontal cylinder embedded in a porous medium. *International Journal of Heat and Mass Transfer*, 1986, **29,** 119–133.
6. Chen, K. S. and Ho, J. R., Effects of flow inertia on vertical natural convection in saturated porous media. *International Journal of Heat and Mass Transfer*, 1986, **29,** 753–759.
7. Plumb, O., The effect of thermal dispersion on heat transfer in packed bed boundary layers. *Proceedings of First ASME and JSME Thermal Engineering Joint Conference*, Vol. 2, 1983, pp. 17–21.
8. Cheng, P., Thermal dispersion effects in non-Darcian convective flows in a saturated porous medium. *Letters to Heat & Mass Transfer*, 1981, **8,** 267–270.
9. Hong, J. T. and Tien, C. L., Analysis of thermal dispersion effect on vertical plate natural convection in porous media. *International Journal of Heat and Mass Transfer*, 1987, **30,** 143–150.
10. Hong, J. T., Yamada, Y. and Tien, C. L., Effects of non-Darcian and non-uniform porosity on vertical plate natural convection in porous media. *Journal of Heat Transfer*, 1987, **109,** 356–361.
11. Cheng, P. and Vortmeyer, D., Transverse thermal dispersion and wall channelling in a packed bed with forced convective flow. *Chemical Engineering Science*, 1988, **43,** 2523–2532.
12. Amiri, A. and Vafai, K., Analysis of dispersion effects and non-thermal equilibrium, non-Darcian, variable porosity incompressible flow through porous media. *International Journal of Heat and Mass Transfer*, 1994, **37,** 939–954.
13. Gebhart, B., Effects of viscous dissipation in natural convection. *Journal of Fluid Mechanics*, 1962, **14,** 225–235.
14. Gebhart, B. and Mollendorf, J., Viscous dissipation in external natural convection flows. *Journal of Fluid Mechanics*, 1969, **38,** 97–107.
15. Fand, R. M. and Brucker, J., A correlation for heat transfer by natural convection from horizontal cylinders that accounts for viscous dissipation. *International Journal of Heat and Mass Transfer*, 1983, **26,** 709–726.
16. Bejan, A., *Convection Heat Transfer*. Wiley, New York 1984, pp. 343–416.
17. Tucker, C. L., III and Dessenberger, R. B., Governing equations for flow and heat transfer in stationary fiber beds. In *Flow and Rheology in Polymer Composites Manufacturing*, ed. S. G. Advani. Elsevier Science, Amsterdam, 1994.
18. Nakayama, A., and Pop, I., Free convection over a non-isothermal body in a porous medium with viscous dissipation. *International Communications in Heat and Mass Transfer*, 1989, **16,** 173–180.